

Barium Titanate Nanoparticles in Block Copolymer

Tu Lee,^{*,†,‡} Nan Yao,[‡] Hiroaki Imai,^{†,‡} and Ilhan A. Aksay^{†,‡}

Department of Chemical Engineering and Princeton Materials Institute, Princeton University, Princeton, New Jersey 08544

Received April 9, 2001. In Final Form: October 2, 2001

Cubic BaTiO₃ particles of ~10 nm were crystallized predominantly within the hydroxylated polybutadiene matrix of a phase separated triblock copolymeric thin film of polystyrene–polybutadiene–polystyrene (Kraton D1102). The barium titanated Kraton thin film had remnants of the cylindrical morphology of a plain Kraton thin film with an interdomain spacing of ~23 nm. The procedure of barium titantation consisted of three steps: (1) in situ hydroxylation of the polybutadiene matrix of an annealed Kraton thin film, (2) regioselective deposition of barium titanium methoxypropanoxide (BaTi(OCH₂CH(CH₂)OCH₃)₆) on the hydroxylated polybutadiene matrix, and (3) hydrothermal reduction of the organometallic complexes in an NH₃/H₂O atmosphere at 80 °C for 24 h. Isolated water clusters in step 3, condensed from the NH₃/H₂O atmosphere of 1 M NH₄OH(aq) at 80 °C in the alkoxide–Kraton films, were believed to have a typical diameter of no more than 23 nm at a pH of 14. They gave a high pH environment to weaken the chelating effect among alkoxides and the organic matrix and provided a spatial confinement for the localized nucleation and growth of cubic BaTiO₃ nanoparticles.

Introduction

The length scales defining structure and organization determine the fundamental characteristics of a material. Unique, size dependent properties are observed especially when the dimensions of a phase, either organic or inorganic, are confined to the nanometer scale (<100 nm).^{1–6} For instance, BaTiO₃, which is used extensively in multilayer capacitors, thermistors, and electrooptic devices,^{7,8} shows a ferroelectric to nonferroelectric phase transition when its size is reduced below 100 nm.^{3,6} The cubic form of BaTiO₃, while not ferroelectric, has a high dielectric constant suitable for capacitors in electronic circuits⁹ despite a relatively low breakdown strength.¹⁰ Consequently, a BaTiO₃/polymer composite is desired in which the breakdown voltage of a ceramic phase is increased by the introduction of a polymer matrix such that the dielectric constant is not compromised.

Nanometer-sized cubic BaTiO₃ particles are commonly crystallized by hydrothermal processing from titanium and barium containing reactants in an aqueous medium under a strongly alkaline condition below 100 °C. Lilley and Wusirika processed monosized powders of cubic

BaTiO₃ by dispersing TiO₂ powders in a concentrated solution of Ba(OH)₂.¹¹ Phule and Risbud precipitated ultrafine (<100 nm) crystalline, cubic BaTiO₃ powders by adding titanyl acylate and barium acetate to a concentrated solution of NaOH.¹² Hydrothermal processing has also been extended to the temperature sensitive BaTiO₃/polymer composite thin films through coprocessing. Slamovich and Aksay spun cast a thin layer (<1 μm) of a compatible mixture of titanium diisopropoxide bis-(ethylacetoacetate) and triblock copolymers of polystyrene–polybutadiene–polystyrene (Kraton D1102) onto a glass substrate and then reacted the film with aqueous solutions of either Ba(OH)₂ or a mixture of NaOH and BaCl₂ at 40–80 °C.¹³

Ideally, a better strategy to engineer the size, shape, and phase of BaTiO₃ particles would be through controlled nucleation and growth in the self-assembling nanodomains of block copolymers: lamellae, cylinders, or spheres at length scales of 10–100 nm.¹⁴ These nanodomains are suited for the design of periodic structures and used to form organic/inorganic nanocomposites.^{15–18} The orientation of nanodomains can also be influenced by the substrate surface. Registration between layers influences the interfacial coordination which propagates into the phase-mixed region. At equilibrium, an organized array is formed everywhere and the periodicity of the nanodomain is well established.^{19–21} Lee and Aksay²² were the first to dem-

* To whom all correspondence should be addressed: Bristol-Myers Squibb Pharmaceutical Research Institute, One Squibb Drive, P. O. Box 191, New Brunswick, NJ 08903-0191. Work: 732-519-1568. Fax: 732-519-3963. E-mail: tu.lee@bms.com.

[†] Department of Chemical Engineering.

[‡] Princeton Materials Institute.

(1) Habib, M. J. *Pharmaceutical Solid Dispersion Technology*; Technomic: PA, 2001. Serajuddin, A. T. M. *J. Pharm. Sci.* **1999**, *88*, 1058. Segal, R. W. *Phys. Today* **1993**, *46*, 64.

(2) Niihara, K. *J. Ceram. Soc. Jpn.* **1991**, *99*, 974.

(3) Lee, T.; Aksay, I. A. *Cryst. Growth Des.* **2001**, *1*, 401. Shih, W. Y.; Shih, W. H.; Aksay, I. A. *Phys. Rev. B* **1994**, *50*, 15575.

(4) Alivisatos, A. P. *Science* **1996**, *271*, 933.

(5) Shi, J.; Gider, S.; Babcock, K.; Awschalom, D. D. *Science* **1996**, *271*, 937.

(6) Uchino, K.; Sadanaga, E.; Hirose, T. *J. Am. Ceram. Soc.* **1989**, *72*, 1555.

(7) Wakino, K.; Mirai, K.; Tamura, H. *J. Am. Ceram. Soc.* **1984**, *67*, 278.

(8) Maurice, A. K.; Buchanan, R. C. *Ferroelectrics* **1987**, *74*, 61.

(9) Kingery, W. D.; Bowen, H. K.; Uhlmann, D. R. *Introduction to Ceramics*, 2nd ed.; Wiley: New York, 1976; Chapter 18.

(10) Ueda, I.; Takiuchi, M.; Ikegami, S.; Sato, H. *J. Phys. Soc. Jpn.* **1964**, *19*, 1267.

(11) Lilley, E.; Wusirika, R. R. Method for the Production of Monosized Powders of Barium Titanate. U.S. Pat. No. 4764493, August, 1988.

(12) Phule, P. P.; Risbud, S. H. *Mater. Sci. Eng.* **1989**, *B3*, 241.

(13) Slamovich, E. B.; Aksay, I. A. *J. Am. Ceram. Soc.* **1996**, *79*, 239.

(14) Hashimoto, T.; Tanaka, H.; Hasegawa, H. *Macromolecules* **1985**, *18*, 1864.

(15) Cummins, C. C.; Beachy, M. D.; Schrock, R. R.; Vale, M. G.; Sankaran, V.; Cohen, R. E. *Chem. Mater.* **1991**, *3*, 1153.

(16) Chan, Y. N. C.; Craig, G. S. W.; Schrock, R. R.; Cohen, R. E. *Chem. Mater.* **1992**, *4*, 885.

(17) Saito, R.; Ishizu, K. *Polymer* **1995**, *36*, 4119.

(18) Spatz, J. P.; Sheiko, S.; Möller, M. *Macromolecules* **1996**, *29*, 3220.

(19) Russell, T. P.; Coulon, G.; Deline, V. R.; Miller, D. C. *Macromolecules* **1989**, *22*, 4600.

(20) Liu, Y.; Zhao, W.; Zheng, X.; King, A.; Singh, A.; Rafailovich, M. H.; Sokolov, J. *Macromolecules* **1994**, *27*, 4000.

(21) Anastasiadis, S. H.; Russell, T. P.; Satija, S. K.; Majkrzak, C. F. *Phys. Rev. Lett.* **1989**, *2*, 1852.

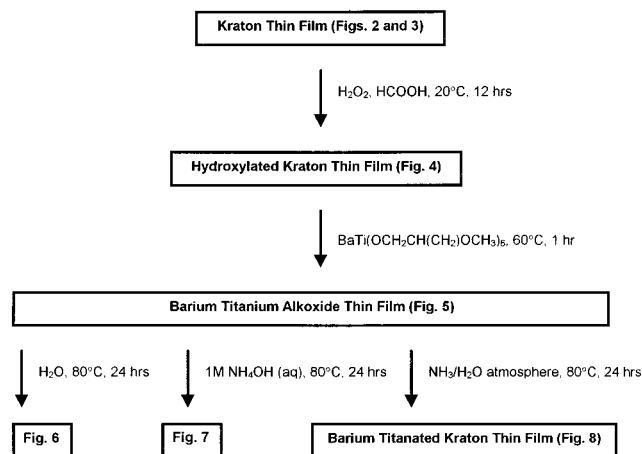


Figure 1. Flowchart of the experimental steps.

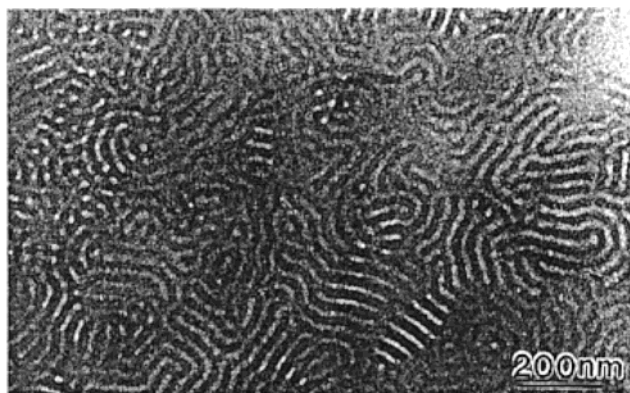


Figure 2. TEM image of the terrace region of the (osmylated stained) annealed thin film of Kraton. The cylinders of polystyrene of ~ 10 nm (light) were in a matrix of polybutadiene of an interdomain spacing of ~ 23 nm (dark). Reprinted with permission from ref 22. Copyright 1997 American Chemical Society.

onstrate the regioselective deposition of barium titanium methoxypropanoxides ($\text{BaTi}(\text{OCH}_2\text{CH}(\text{CH}_3)\text{OCH}_3)_6$) within the hydroxylated polybutadiene matrix of the Kraton D1102 thin film (alkoxide–Kraton thin film). Although the alkoxide–Kraton thin film exhibited a cylindrical morphology with an interdomain spacing of ~ 23 nm, crystalline BaTiO_3 was not observed to result when the alkoxide–Kraton thin film was reacted with an alkaline solution.

Therefore, the aim of this study is to propose a hydrothermal process for crystallizing the alkoxide–Kraton thin film in our previous work²² without compromising its pattern. To develop the novel hydrothermal method, it is necessary to investigate the chemical and morphological behaviors of the alkoxide–Kraton thin films in (1) H_2O , (2) 1 M $\text{NH}_4\text{OH}(\text{aq})$, and (3) the $\text{NH}_3/\text{H}_2\text{O}$ atmosphere of a 1 M $\text{NH}_4\text{OH}(\text{aq})$ solution.

The flowchart of the experimental steps shown in Figure 1 reviews what we have accomplished in our previous work²² (Figures 2–5 in ref 22) and summarizes its connection to our present study. The TEM image in Figure 2 reveals that the Kraton thin film has cylindrical polystyrene (PS) nanodomains with a spacing of 10 nm which are embedded in a polybutadiene (PB) matrix with an interdomain spacing of 23 nm. Figure 3 depicts a three-dimensional, ~ 50 nm thick, monolayered Kraton thin film

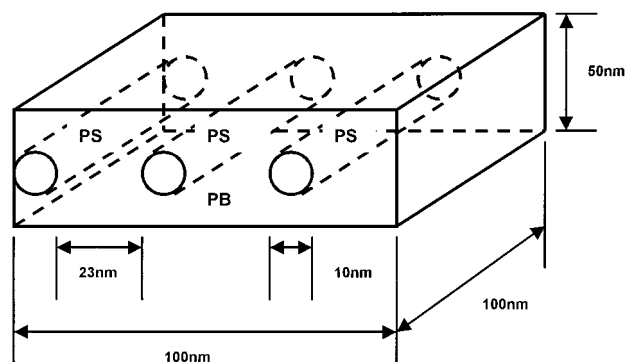


Figure 3. Schematic diagram of a $100 \text{ nm} \times 100 \text{ nm} \times 50 \text{ nm}$ Kraton thin film: PS, polystyrene cylinders; PB, polybutadiene matrix.

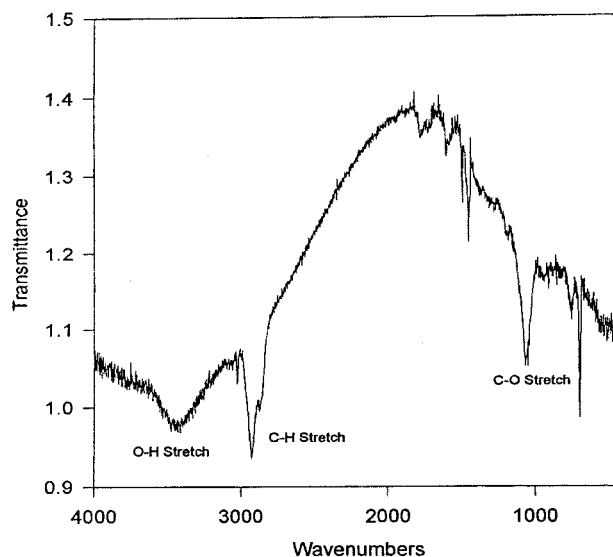


Figure 4. Transmission FTIR spectrum of the hydroxylated thin film of Kraton which did not have any contrast under a TEM.

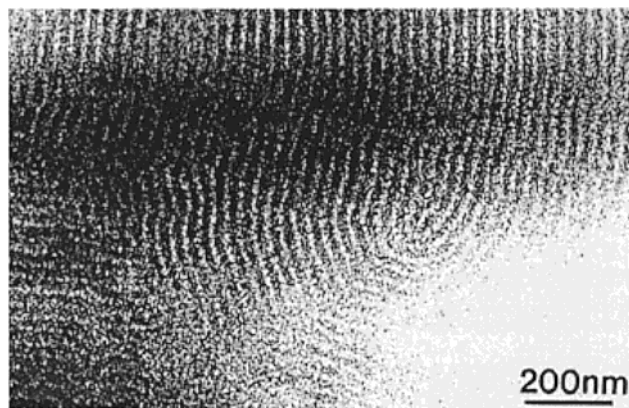


Figure 5. TEM image of the terrace region of the coordinated barium titanium double alkoxide doped thin film of Kraton. The cylindrical nanodomain spacing of PS (light) was ~ 10 nm, and the barium titanated interdomain spacing (dark) was ~ 23 nm.

as measured by ellipsometry. Upon hydroxylation, the PB matrix of the Kraton thin film is OH-functionalized as shown by the broad OH stretching band near $3400\text{--}3600 \text{ cm}^{-1}$ measured by the transmission FTIR (Figure 4). After barium titanation, the alkoxide–Kraton thin film still exhibits a cylindrical morphology with an interdomain spacing of ~ 23 nm (Figure 5). Figures 2, 4, and 5 were discussed in great detail in our previous work.²²

(22) Lee, T.; Yao, N.; Aksay, I. A. Nanoscale Patterning of Barium Titanate on Block Copolymers. *Langmuir* **1997**, *13*, 3866.

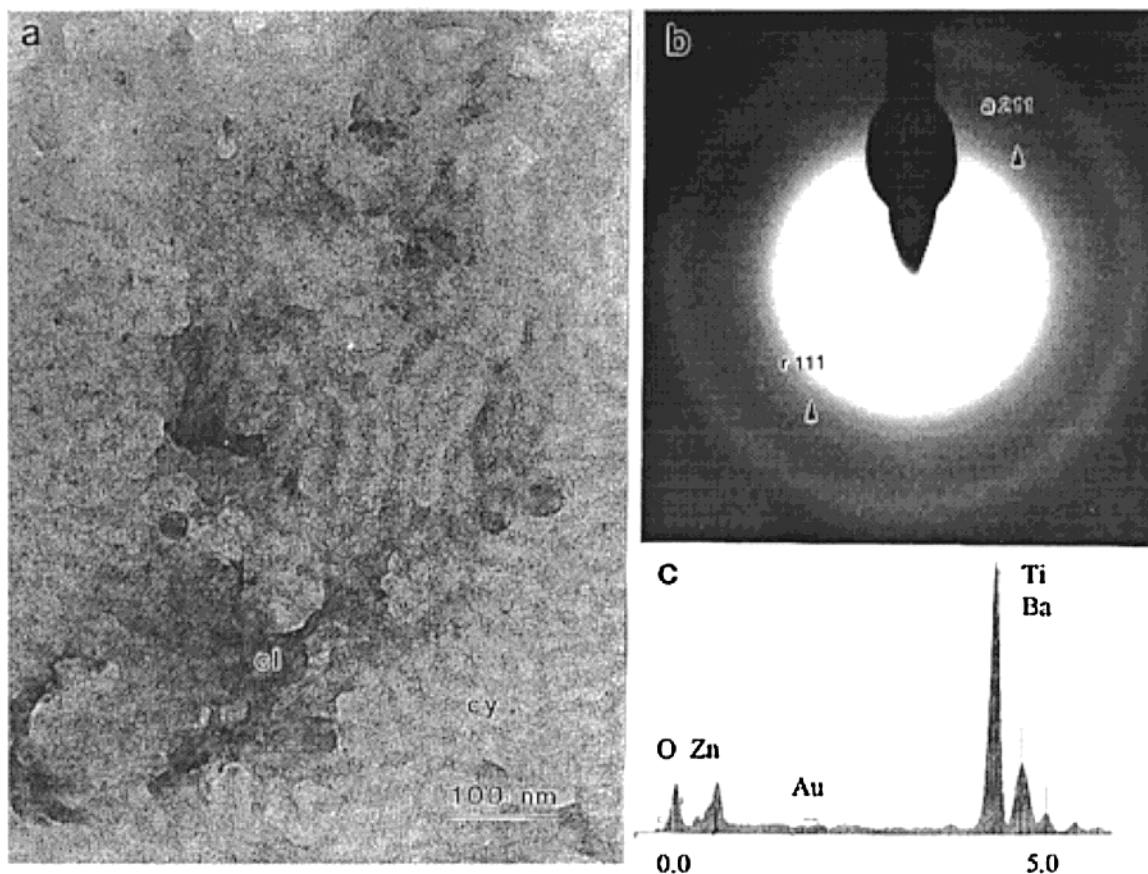


Figure 6. Alkoxide-Kraton thin film after H₂O immersion: (a) TEM image; (b) selected-area diffraction pattern of [cy] in part a; (c) EDS spectrum of [cy] in part a; [cy], the original cylindrical morphology; [cl], cloudy morphology; [a], anatase TiO₂; [r], rutile TiO₂.

Experimental Procedures

General Methods. To minimize the formation of solid BaCO₃ from the reaction between liquid barium titanium methoxypropanoxide (BaTi(OCH₂CH(CH₃)OCH₃)₆, containing 2.0–2.2 wt % Ti and 5.7–6.0 wt % Ba, metal ratio Ba/Ti = 1:1, density = 0.98–1.01) (Gelest Inc., Tullytown, PA) and gaseous CO₂, double distilled H₂O used in all aqueous solutions was boiled for 30 min to remove dissolved CO₂. All bottles with reactants were purged with N₂, sealed, and kept in an oven at 80 °C for 24 h at 1 atm. Polyethylene bottles and scintillating vials were utilized to avoid silicon and aluminum contamination from glassware at high pH. NH₄OH(aq) rather than other strong bases such as NaOH or KOH was used to provide a basic condition not only for the liquid phase but also for the vapor phase. This is because NH₄OH(aq) can be evaporated into H₂O vapor and be decomposed into alkaline NH₃ gas simultaneously upon heating.

Alkoxide-Kraton thin films were prepared as follows:²² Thin (<50 nm) films of polystyrene (PS)-polybutadiene (PB)-polystyrene (PS), Kraton D1102 (fractionated Kraton: MW ~ 35 000 g/mol, Block MW ~ 4900 (PS)-25 200 (PB)-4900 (PS)) (Shell Chemical Company, Houston, TX), were made by spin casting (Spin coater; Model No. CB 15, Headaway Research Inc., Garland, TX) a 1 wt % Kraton/toluene solution with a rotational speed of 2500 rpm on a 22 mm × 22 mm cover glass which had previously been spun cast with a layer of 10 vol % aqueous detergent solution (Mr. Clean, Protor and Gamble, Cincinnati, OH) and coated with a layer of ~7 nm thick amorphous carbon. Film thicknesses were measured by ellipsometry (Model No. L116C, Gaertner Inc., Chicago, IL). Films were scored into small pieces with a diamond knife and lifted off from the cover glass surface by dipping the film-coated cover glass into double distilled water. Gold transmission electron microscope (TEM) specimen grids (SPI Supplies, West Chester, PA) were then used to pick up the floating Kraton thin films, and the samples were annealed for 24 h at 130 °C under vacuum to obtain phase separation. The annealed thin films of Kraton on gold TEM grids were then

epoxidized-hydroxylated in 0.974 g of 85 wt % formic acid (J.T. Baker, Phillipsburg, NJ) to which 2.04 g of 30 wt % hydrogen peroxide (J.T. Baker, Phillipsburg, NJ) was slowly added within 2 h below 20 °C.²³ The mixture was agitated by a stream of N₂ for 10 h more below 20 °C. The hydroxylated samples were vacuum-dried and then reacted with BaTi(OCH₂CH(CH₃)OCH₃)₆ under dry N₂ for 1 h at 60 °C. The reaction was then terminated by rinsing the alkoxide-Kraton samples with copious amounts of *n*-butanol (J.T. Baker, Phillipsburg, NJ) at room temperature.

Thin films were examined by analytical TEMs (CM20 and CM200 FEG Philips Electronic Instruments, Mahwah, NJ), and the quantitative measurements of barium, titanium, and oxygen were analyzed by energy-dispersive spectroscopy (EDS) (Princeton Gamma-Tech., Princeton, NJ) using a 5 nm electron probe. Bulk particles were analyzed by powder X-ray diffraction (XRD) (Scintag Sieman D500). Cu K α radiation and a scan rate of 1.2°/min from 20 to 80° 2 θ were used.

(1) In H₂O. The alkoxide-Kraton thin film was immersed in 10 mL of H₂O contained in a capped bottle.

(2) In 1 M NH₄OH(aq). The alkoxide-Kraton thin film was immersed in 10 mL of 1 M NH₄OH(aq) contained in a capped bottle.

(3) In an NH₃/H₂O Atmosphere. The alkoxide-Kraton film was placed on a piece of filter paper in an open scintillating vial which was floated on 10 mL of 1 M NH₄OH(aq) contained in a capped bottle.

Results and Discussion

In experiment 1, the original cylindrical morphology (Figure 5) of the alkoxide-Kraton thin film [cy] (Figure 6a) was partially evolved into a cloudy morphology [cl] (Figure 6a). The cylinder-like region [cy] was mainly amorphous and had traces of anatase TiO₂ [a] and rutile

(23) Kalfoglou, N. K.; Margaritis, A. G. *Eur. Polym. J.* **1988**, *24*, 1043.

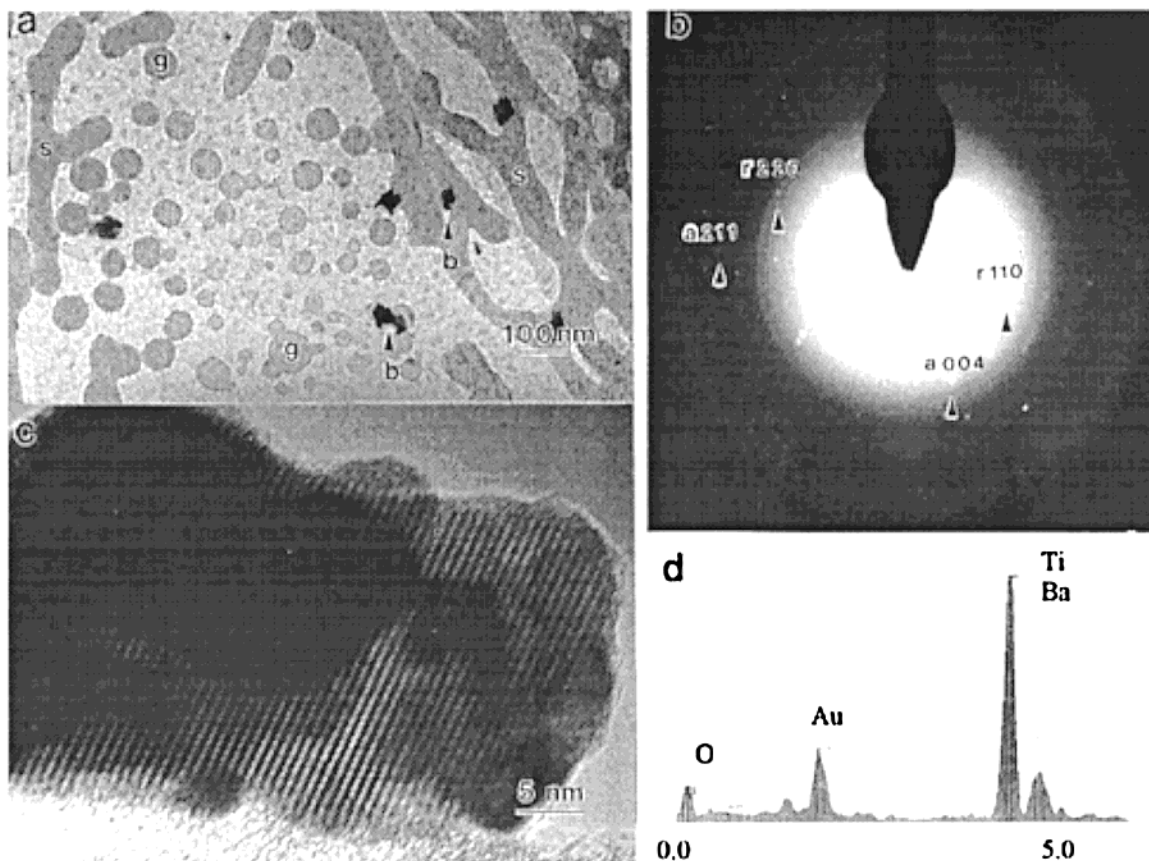


Figure 7. Alkoxide-Kraton thin film after 1 M $\text{NH}_4\text{OH}(\text{aq})$ immersion: (a) TEM image; (b) selected-area diffraction pattern of [s] and [g] in part a; (c) high-resolution TEM image of [b] in part a; (d) EDS spectrum of [s] in part a with $d_{110} = 2.85 \text{ \AA}$; [s], serpentine morphology; [g], globular morphology; [b], cubic BaTiO_3 particle; [a], anatase TiO_2 ; [r], rutile TiO_2 .

TiO_2 [r] (Figure 6b). The cylinder-like region [cy] in Figure 6a had the atomic percent values of Ba, Ti, and O of 22.76, 18.16, and 59.08, respectively (Figure 6c).

The cylinder-like pattern [cy] in Figure 6a, however, was totally defaced in experiment 2 (Figure 7a) by amorphous Ba-Ti-Kraton serpentine [s] and globular [g] morphologies having traces of anatase TiO_2 [a] and rutile TiO_2 [r] (Figure 7b). The film was partially scattered with 50–100 nm cubic BaTiO_3 particles [b] (Figure 7a) with $d_{110} = 2.85 \text{ \AA}$.²⁴ The amorphous serpentine [s] domain in Figure 7a had the atomic percent values of Ba, Ti, and O of 21.43, 17.86, and 60.71, respectively (Figure 7d).

In experiment 3, the thin film in Figure 8a had remnants of the original cylindrical morphology of alkoxide-Kraton with an interdomain spacing of 23 nm (Figures 5 and 6a [cy]). Cubic BaTiO_3 nanoparticles [b] (Figure 8a) of ~ 10 nm were formed and located predominantly within the hydroxylated polybutadiene matrix [t] (Figure 8a). The selected-area diffraction pattern in Figure 8b further showed that the cylinder-like region [t] in Figure 8a is composed of polycrystalline cubic BaTiO_3 . BaTiO_3 particles [b] in Figure 8a had the atomic percent values of Ba, Ti, and O of 23.92, 17.39, and 58.69, respectively (Figure 8c).

The mass balance of Ba and Ti species among the Kraton thin film, the 7 nm thick supporting amorphous carbon thin film, and the supernatant will not be considered because the exact uptake of alkoxide by the amorphous carbon thin film was not determined. Major results of all experiments are summarized in Table 1.

Ideally, experiment 1 should have produced BaTiO_3 particles because (1) BaTiO_3 particles could be formed

experimentally by reacting barium titanium methoxypropanoxide with water (the resulting pH of the mixture > 7) (Figure 9), and (2) the concentration of Ba species in the film gave a $\log m_{\text{Ba}} = -5.7$ and a pH of 14 (Appendix I), which satisfied the stability diagram outlining the required concentration and pH for synthesizing cubic BaTiO_3 particles among other materials derived by Lencka and Riman,²⁵ who performed calculations defining the thermodynamics of hydrothermal processing (Figure 10).

But the absence of BaTiO_3 in experiment 1 suggested that the chelating effect among alkoxides and hydroxylated Kraton (Figure 11),²⁶ which Lencka and Riman's original stability diagram (Figure 10) did not account for among all other possible reactions which might occur in the hydrothermal medium, prohibited the crystallization of BaTiO_3 . Since metal alkoxides were known to react with dihydroxy alcohols such as glycols to form highly polymeric glycolate derivatives which had resistance to hydrolysis,^{26–28} the chelating effect was thought to be responsible for the stabilization of Ba and Ti sources in the film even with the presence of water.^{29–31}

Figure 11 showed that there were two possible ways to form chelating coordination. Structure I mainly involved a tetracoordinated titanium atom from the $\text{BaTi}(\text{OR})_6$

(25) Lenka, M. M.; Riman, R. E. *Chem. Mater.* **1993**, *5*, 61.

(26) Reeves, R. E.; Mazzeno, L. W. *J. Am. Chem. Soc.* **1954**, *76*, 2533.

(27) Chaibi, J.; Henry, M.; Zarrouk, H.; Gharbi, N.; Livage, J. *J. Non-Cryst. Solids* **1994**, *170*, 1.

(28) Yamamoto, Y.; Kambara, S. *J. Am. Chem. Soc.* **1959**, *81*, 2663.

(29) Sanchez, C. *J. Noncryst. Solids* **1992**, *147 & 148*, 1.

(30) Antonelli, D. M.; Ying, J. Y. *Angew. Chem., Int. Ed. Engl.* **1995**, *34*, 2014.

(31) Wada, S.; Kubota, A.; Suzuki, T.; Noma, T. *J. Mater. Sci. Lett.* **1994**, *13*, 190.

(24) Bursill, L. A.; Peng, J.; Fan, X. *Ferroelectrics* **1989**, *97*, 71.

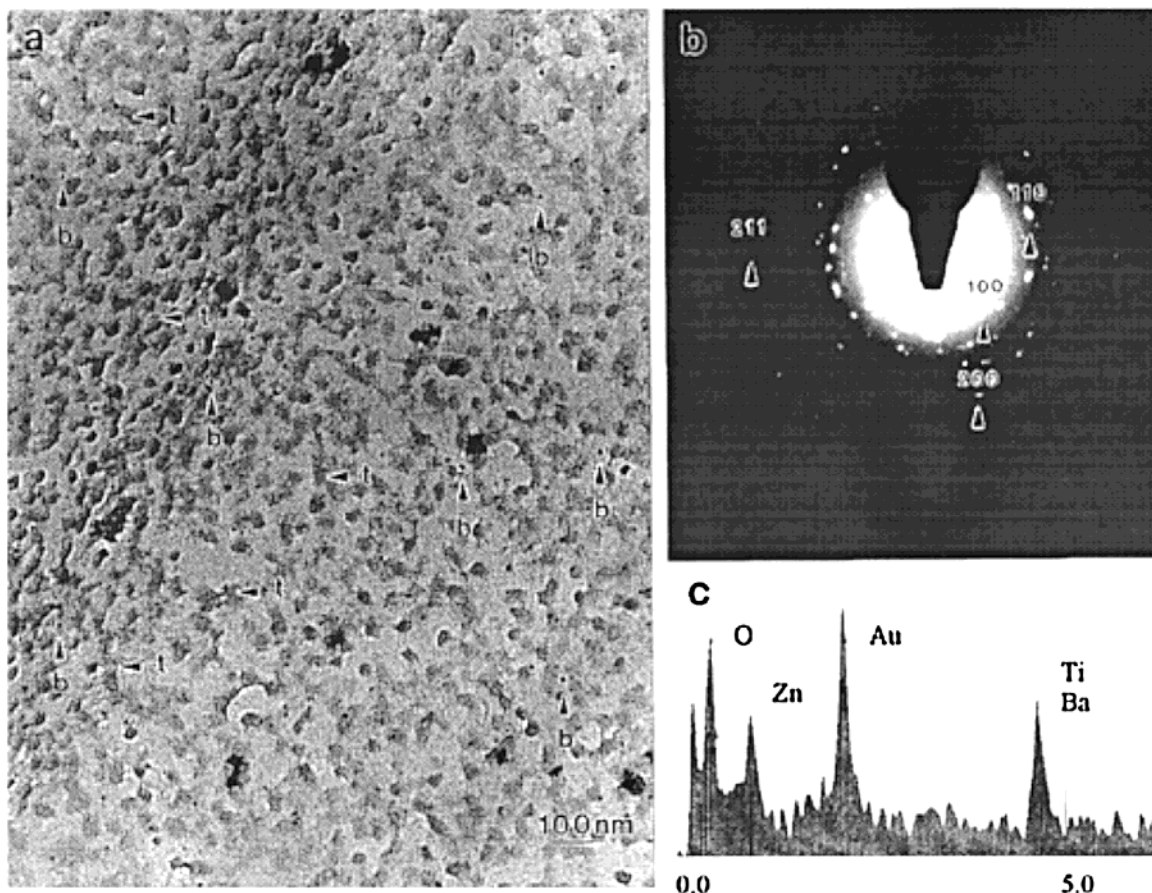


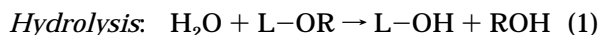
Figure 8. Alkoxide–Kraton thin film treated with $\text{NH}_3/\text{H}_2\text{O}$ atmosphere: (a) TEM image; (b) selected-area diffraction pattern of [b] in part a; (c) EDS spectrum of [b] in part a; [t], *trans*-1,2-polybutadiol matrix; [b], cubic BaTiO_3 nanoparticles.

Table 1. Morphology and Crystallinity of Hydrothermally Treated Barium–Titanium–Methoxypropanoxide–Kraton Films in Liquid and Vapor Media at 80 °C for 24 h

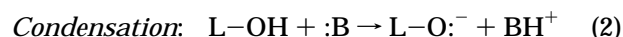
experiment	morphology	crystallinity	atom%		
			Ba	Ti	O
1 in H_2O	partially cloudy	amorphous Ba–Ti–Kraton anatase TiO_2 and rutile TiO_2	22.76	18.16	59.08
2 in 1 M $\text{NH}_4\text{OH}(\text{aq})$	serpentine and globular	amorphous Ba–Ti–Kraton anatase TiO_2 , rutile TiO_2 , and cubic BaTiO_3	17.86	21.43	60.71
3 in $\text{NH}_3/\text{H}_2\text{O}$ atmosphere of 1 M $\text{NH}_4\text{OH}(\text{aq})$	cylinder-like	polycrystalline cubic BaTiO_3	23.92	17.39	58.69

complex bound to two hydroxyl groups on each of two polymer chains while structure II mainly involved a hexacoordinated titanium atom from the $\text{BaTi}(\text{OR})_6$ complex bound to three hydroxyl groups on each polymer chain.²⁶ However, the coordinated titanium species were susceptible to the attack of liquid H_2O only to a certain degree, and yet the hydrolyzed moieties might be recondensed immediately with the hydroxylated Kraton matrix, as evidenced by the morphological transformation from cylinders to cloudiness.

Although the local concentration of Ba species (Appendix I) in the film would have given a pH of 14 under normal conditions, the chelating effect suppressed the hydrolysis of Ba species and the dissociation of $\text{Ba}(\text{OH})_2$. Consequently, the local pH was only high enough for the formation of traces of TiO_2 ²⁵ but not high enough for the complete weakening of the chelated structure of alkoxide–Kraton²⁹ to fabricate cubic BaTiO_3 .²⁵ The role of H_2O was believed to first hydrolyze the alkoxides by forcing out the alkoxide ligands via nucleophilic substitution



where L = hydrolyzed alkoxide oligomer, Ba or Ti, and R = $\text{OCH}_2\text{CH}(\text{CH}_3)\text{OCH}_3$ and Kraton matrix, whereas the role of the alkaline condition was to produce strong nucleophiles (L-O^-) via deprotonation of hydroxo ligands



where L = hydrolyzed alkoxide oligomer, Ti or H, and B = :OH^- or NH_3 , so that condensation among L-O^- and L-OH species could take place.^{32,33} Therefore, a higher pH condition achieved by the addition of foreign nucleophilic OH^- ions was desired to weaken the chelating effect among alkoxides and the organic matrix. This was illustrated by Calvert and Broard, who, unable to form cubic BaTiO_3 from barium–titanium-mixed-alkoxide/poly-(butyl methacrylate) composites solely by hydrolysis, were able to do so in a saturated $\text{Ba}(\text{OH})_2$ solution.³⁴ This was

(32) Klee, M. *J. Mater. Sci. Lett.* **1989**, *985*, 8.

(33) Brinker, C. J.; Scherer, G. W. *Sol–Gel Science*; Academic Press: London, U.K., 1989; pp 21–95.

(34) Calvert, P.; Broard, A. *Mater. Res. Soc. Symp. Proc.* **1990**, *174*, 61.

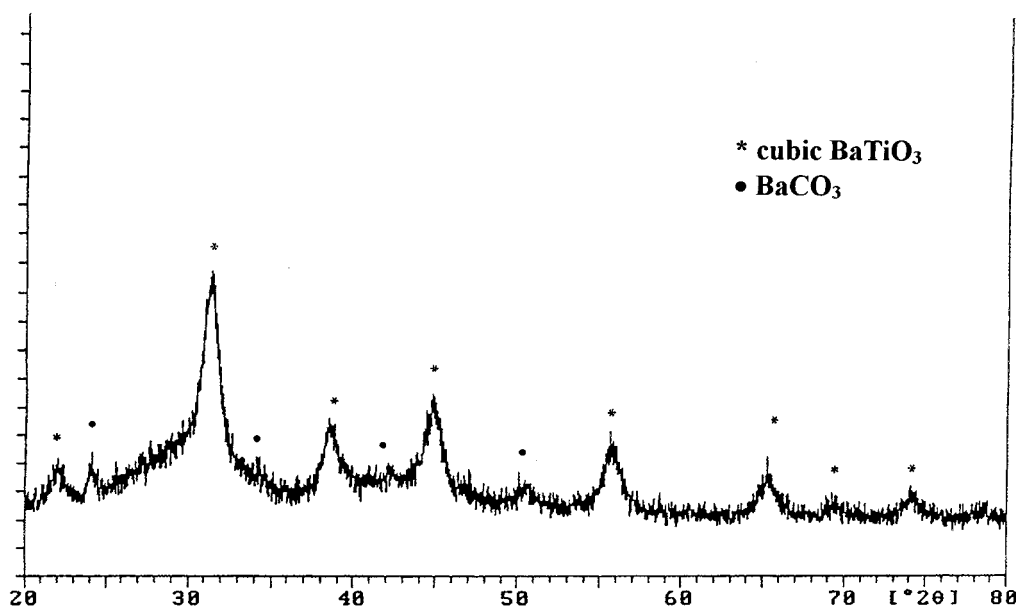


Figure 9. Typical X-ray diffraction pattern of cubic BaTiO_3 particles formed by reacting 2 g of $\text{BaTi}(\text{OCH}_2\text{CH}(\text{CH}_3)\text{OCH}_3)_6$ with 10 mL of H_2O at 80°C for 24 h.

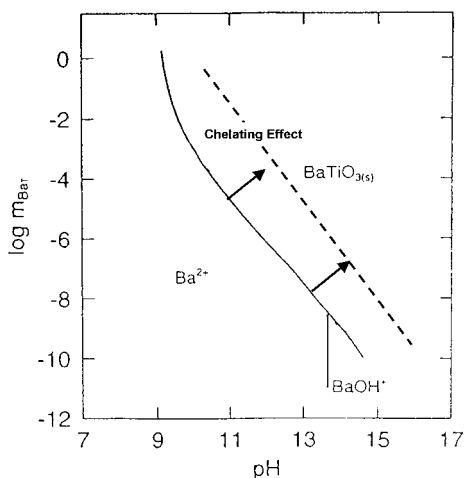


Figure 10. Calculated stability diagram for the Ba system at 363.15 K using modeled activity coefficients. The dashed line was added to show the chelating effect.

also proven in experiment 2, where complete morphological deformation and some formation of cubic BaTiO_3 particles were observed upon the addition of 1 M $\text{NH}_4\text{OH}(\text{aq})$.

The interplay between chelation (Figure 11) and hydrolysis–condensation (eqs 1 and 2) has led us to propose the hopping mechanism (Figure 12) which was derived from Figure 11. It was a continuous cyclic process of step 1 to step 5. In step 1, the chelated structure of the coordinated barium–titanium–*trans*-1,2-polybutadiol chains in the Kraton matrix was under the $\text{S}_{\text{N}}2$ nucleophilic attack of the hydroxyl ions. In step 2, condensed bonds were partly broken by an exchange reaction of the chelated hydroxyl sites with the hydroxyl ions. The liberated Ba and Ti species were migrating to the next chelated hydroxyl sites. In step 3, Ti species interacted with the nearby chelating hydroxyl sites in the hydroxylated polybutadiene matrix by a hexacoordination. In step 4, the exchange reaction was taking place among the hydroxyl groups on Ba and Ti species and the chelated hydroxyl groups in the hydroxylated polybutadiene matrixes. In step 5, the Ba and Ti species were condensed again at a new position in the hydroxylated polybutadiol matrix. The hopping mechanism was the mode of trans-

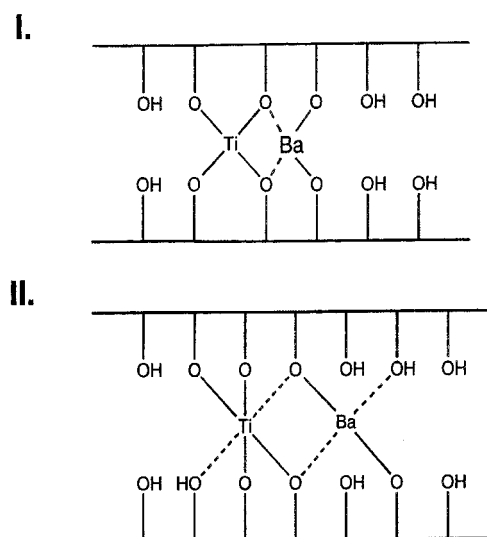


Figure 11. Chelate structure formed between $\text{BaTi}(\text{OCH}_2\text{CH}(\text{CH}_3)\text{OCH}_3)_6$ and *trans*-1,2-polybutadiol chains (represented schematically by the horizontal lines) in the Kraton matrix: structure I, tetracoordination; structure II, hexacoordination.

portation in the film, and it was related to the formation of traces of TiO_2 , the morphogenesis of the amorphous alkoxide–Kraton network, and the migration of Ba and Ti species in the film.

For example, the amorphous serpentine Ba and Ti rich rods in Figure 7a were the manifestation of the diffusion of shorter Ba–O–Ti oligomers in the film by the hopping mechanism. The orientation of the rods might be dictated by the higher diffusivity parallel to the interface of the cylindrical polystyrene nanodomain in the film.³⁵ As the Ba–O–Ti oligomers grew into longer polymers by hydrolysis–condensation, the suppression on the diffusion due to chelation became stronger and clustering of like Ba–O–Ti polymers took place.³⁶ To decrease the surface

(35) Luther, E. P.; Chun, C. M.; Lee, T.; Aksay, I. A. *Advances in Dielectric Ceramic Materials*; Nair, K. M., Bhalla, A. S., Eds.; The American Ceramic Society: Westerville, OH, 1998; pp 189–194.

(36) Kannan, R. M.; Su, J.; Lodge, T. P. *J. Chem. Phys.* **1998**, *108*, 4634.

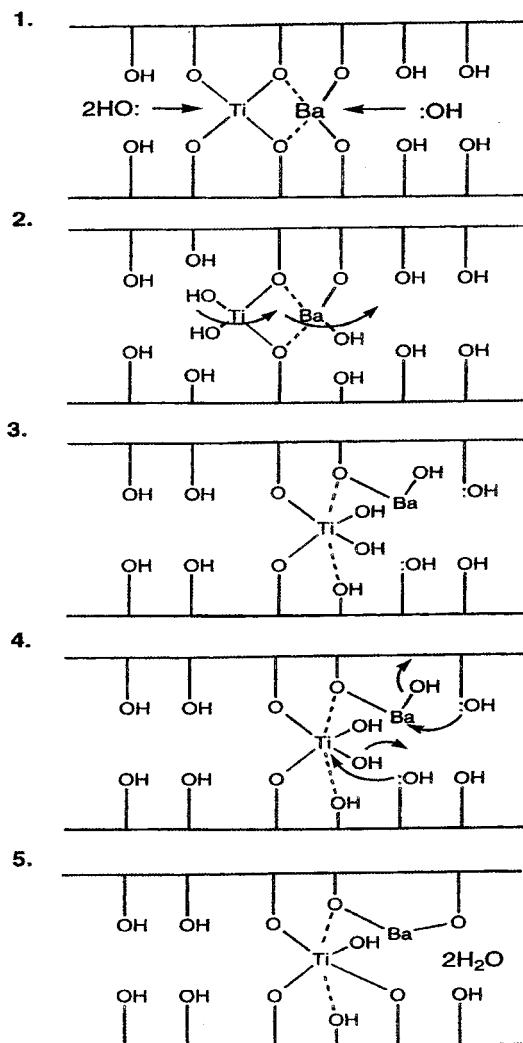


Figure 12. Hopping mechanism.

tension and attain the most thermodynamically stable configuration, circular globules were formed in the film (Figure 7b).

Cubic BaTiO_3 particles in experiment 2 (Figure 7a) were believed to be formed on the surface of the alkoxide–Kraton thin film because the dimension of the particles of ~ 50 – 100 nm was larger than the film thickness of ~ 50 nm. The ability to nucleate particles directly from the amorphous alkoxide–Kraton thin film suggested that a dissolution–precipitation mechanism¹³ might be operative. Similar to the formation of a BaTiO_3 thin film on a Ti substrate,³⁷ the formation of BaTiO_3 particles on the Ba and Ti rich alkoxide–Kraton thin film might consist of the following seven steps: (1) permeation of 1 M $\text{NH}_4\text{OH}(\text{aq})$ in the film, (2) dissolution of Ba and Ti species in the film through hydrolysis in 1 M $\text{NH}_4\text{OH}(\text{aq})$, (3) generation of Ba and Ti ions, (4) transport of Ba and Ti ions to the plane exposed by the dissolution, (5) adsorption of Ba and Ti ions on the film surface, (6) nucleation, and (7) growth of the crystalline particle. According to the hopping mechanism, cubic BaTiO_3 particles should be nucleated and nested near the sites where the local concentration of Ba–O–Ti polymers, which were vulnerable to the attack of OH^- ions, was high. The termination of growth occurred when freely moving Ba and Ti ions were consumed. Theoretically, the population of particles

was $\sim 2.3 \times 10^5$ (Appendix II). The observation of particles appearing first on the alkoxide–Kraton thin film surface was consistent with heterogeneous nucleation, which occurred preferentially at the free surface.

Lessons from experiments 1 and 2 indicated that cubic BaTiO_3 nanoparticles and barium titanated Kraton thin films exhibiting cylindrical morphology might be obtained if (1) the pH of the water was high enough to liberate all the Ba and Ti species from the chelate alkoxide–Kraton structure and (2) the continuous pool of water in the film was discretely compartmentalized and miniaturized so that the formation of amorphous Ba–Ti rods can be eliminated. These two requirements could be satisfied simultaneously by exposing the alkoxide–Kraton thin films to an $\text{NH}_3/\text{H}_2\text{O}$ atmosphere which was based on hydrolysis of alkoxide coatings using water vapor.^{38,39}

In experiment 3, at the temperature 80°C , the partial pressure of $\text{NH}_3(\text{g})$ in the $\text{NH}_3/\text{H}_2\text{O}$ atmosphere of 1 M $\text{NH}_4\text{OH}(\text{aq})$ was 349 mmHg and the amount of $\text{NH}_3(\text{g})$ dissolved in H_2O vapor was 5 wt %.⁴⁰ The resulting alkaline condensate had an $\text{NH}_3(\text{g})$ concentration of 3 M and a pH of 14. In contrast to the cloudy amorphous Ba–Ti morphology obtained in experiment 1, the remnants of the cylindrical morphology of the alkoxide–Kraton thin films in experiment 2 implied that the high pH water condensate was not in the form of a continuous pool. In addition, BaTiO_3 particles with a size of around 10 nm implied that the high pH water condensate was in the form of water clusters of ~ 10 – 23 nm in which BaTiO_3 particles nucleated and grew. The inference of the presence of water clusters agreed closely with the work of Salmeron and co-workers.⁴¹ They had used the polarization force between an electrically charged atomic force microscope tip and a substrate to follow the process of condensation and evaporation of a monolayer of water on mica at room temperature; and they had shown that, up to about 25% humidity, many two-dimensional clusters with typical diameters of 10 nm and apparent heights of ~ 2 Å were initially formed.

Similar to experiment 2, the formation of BaTiO_3 particles in experiment 3 might consist of the following seven steps: (1) permeation of high pH water vapor in the film, (2) formation of water clusters by high pH water vapor condensation in the hydrophilic region of the hydroxylated Kraton matrix, namely, the hydroxylated polybutadiene region, (3) dissolution of Ba and Ti species in water clusters through hydrolysis, (4) generation of Ba and Ti ions in water clusters, (5) nucleation, and (6) growth of the crystalline particle.

Water clusters in the film served as a spatial confinement for the formation and growth of cubic BaTiO_3 nanoparticles by the dissolution–precipitation mechanism.⁴² Theoretically, there was one 10 nm spherical BaTiO_3 particle per area of $380 \text{ nm} \times 380 \text{ nm}$ (Appendix II). The hydroxyl group in the thin film and the disordered region at the interface⁴³ of hydroxylated polybutadiene–polystyrene might act as a nucleation site. The necking of some BaTiO_3 rich nanodomains (Figure 8a) suggested

(38) Matsuda, A.; Kogure, T.; Matsuno, Y.; Katayama, S.; Tsuno, T.; Tohge, N.; Minami, T. *J. Am. Ceram. Soc.* **1993**, *76*, 2899.

(39) Matsuda, A.; Matsuno, Y.; Katayama, S.; Tsuno, T.; Tohge, N.; Minami, T. *J. Ceram. Soc. Jpn.* **1994**, *102*, 330.

(40) Perry, R. H.; Green, D. W.; Maloney, J. O. *Perry's Chemical Engineers' Handbook*, 6th ed.; McGraw-Hill: New York, 1985.

(41) Hu, J.; Xiao, X. D.; Ogletree, D. F.; Salmeron, M. *Science* **1995**, *268*, 267.

(42) Chun, C. M.; Navrotsky, A.; Aksay, I. A. *Proc. Microscopy and Microanalysis 1996*; Bailey, G. W., Corbett, J. M., Dimlich, R. V. W., Michael, J. R., Zaluzec, N. J., Eds.; San Francisco Press: San Francisco, CA, 1996; pp 656 and 676.

(43) Aizenberg, J. *J. Chem. Soc., Dalton Trans.* **2000**, 3963.

(37) Shi, E.; Cho, C. R.; Jang, M. S.; Jeong, S. Y.; Kim, H. J. *J. Mater. Res.* **1994**, *9*, 2914.

that water clusters carrying ions, alkoxide oligomers, or even small BaTiO₃ particles could migrate through the polymer before creating or reaching a nucleation site.⁴⁴ But the exact diffusion path, that is whether the materials diffused through the interdomains of hydroxylated polybutadiene, the nanodomains of polystyrene, or the interfaces of hydroxylated polybutadiene–polystyrene,³⁶ is not known at this point. The diffusion of materials in films was enhanced by the temperature 80 °C, localized heating, and volume changes in the materials caused by the exothermic reduction process. The size of the BaTiO₃ particle was also limited by the local concentration of alkoxides, given a mixed number of nucleation sites. The very similar kinds of morphological phenomena mentioned above were observed by Cohen and co-workers in the formation of small palladium and platinum nanoclusters within nano-phase-separated diblock copolymers.¹⁶

Further studies on the effect of reaction temperature, time, and pH on the morphogenesis and the crystallinity of the alkoxide–Kraton thin films will be necessary to optimize the hydrothermal process in the NH₃/H₂O atmosphere.

Conclusion

The hydrothermal processing of barium–titanium–methoxypropanoxide–Kraton thin films in the NH₃/H₂O atmosphere of 1 M NH₄OH(aq) at 80 °C provided a feasible way to synthesize cubic BaTiO₃ particles of ~10 nm inside the interdomains of a Kraton thin film with the remnants of cylindrical morphology of the alkoxide–Kraton thin film. This approach spatially confined the nucleation and growth of cubic BaTiO₃ particles in high pH, ammonia-conditioned water clusters. Most likely, the water clusters were isolated from each other, were located in the hydroxylated polybutadiene matrixes, and had sizes of no more than 23 nm. An extremely alkaline environment was needed to completely weaken the Ba–Ti–Kraton chelated structure formed among alkoxides and the hydroxylated polybutadiene matrix. Consequently, Lencka and Riman's stability diagram²⁵ for the Ba–Ti system was inapplicable to this Ba–Ti–Kraton system unless the interaction among alkoxides and the hydroxylated Kraton was also included in all possible reactions that might occur in the hydrothermal medium. Ba and Ti species were believed to migrate in the Kraton matrix by a hopping mechanism. The merging of BaTiO₃ clusters suggested that water clusters carrying ions, alkoxide oligomers, and small BaTiO₃ clusters could travel through the polymer.

Acknowledgment. This work was supported by a grant from the Army Research Office (DAAL03-92-G-0241) and the MRSEC program of the National Science Foundation (DMR-940032). Suggestions from Dr. D. H. Ad-

amson and the assistance of Dr. C. M. Chun are gratefully acknowledged.

Appendix I

The mole/mole uptake ratio, y , of barium titanium double alkoxide in all the films was experimentally determined to be 0.05 by the weight gain of a bulk hydroxylated Kraton in barium titanium double alkoxide at 80 °C for 1 h. Assuming the film was saturated with liquid water everywhere, the total molal concentration of Ba and Ti species in the film, m , can be approximated as

$$m = y \frac{\rho_{\text{PB}}}{\text{MW}_{\text{PB}} \rho_{\text{H}_2\text{O}}} \times 1000 \text{ mol/kg}$$

where the density of polybutadiene $\rho_{\text{PB}} = 0.97 \text{ g/cm}^3$, the uptake ratio $y = 0.05$, the weight-average molecular weight of polybutadiene $\text{MW}_{\text{PB}} = 25\,200 \text{ g/mol}$, and the density of water $\rho_{\text{H}_2\text{O}} = 1 \text{ g/cm}^3$. Therefore, $m = 1.9 \times 10^{-6} \text{ mol/kg}$ and $\log m_{\text{Ti}} \sim \log m_{\text{Ba}} = -5.7$.

Since Ba(OH)₂ was one of the hydrolyzed derivatives from barium titanium double alkoxide³² and if the equilibrium of Ba(OH)₂(s) = Ba²⁺(aq) + 2OH⁻(aq) was fully established inside the films, based on the solubility product, $K_{\text{sp}}(80 \text{ °C}) = 9.09 \times 10^{-6}$ extrapolated from $K_{\text{sp}}(25 \text{ °C}) = 2.55 \times 10^{-6}$ by the Van't Hoff equation, the local pH in the film should be 14.

Appendix II

Since the volume of the 100 nm × 100 nm × 50 nm Kraton patch in Figure 3 is $5 \times 10^{-6} \text{ cm}^3$ and the volume of each PS cylinder is $\sim 7.9 \times 10^{-18} \text{ cm}^3$, the volume of the PB matrix is $4.76 \times 10^{-16} \text{ cm}^3$. The number of moles of PB, n_{PB} , in the patch is calculated as

$$n_{\text{PB}} = \frac{\rho_{\text{PB}} V_{\text{PB}}}{\text{MW}_{\text{PB}}}$$

where the density of polybutadiene $\rho_{\text{PB}} = 0.97 \text{ g/cm}^3$, the volume of polybutadiene $V_{\text{PB}} = 4.76 \times 10^{-16} \text{ cm}^3$, and the weight-average molecular weight of polybutadiene $\text{MW}_{\text{PB}} = 25\,200 \text{ g/mol}$. Therefore, $n_{\text{PB}} = 1.83 \times 10^{-20} \text{ mol}$. Since the uptake ratio for Ba and Ti species is 0.05, the number of moles of Ba and Ti atoms is $9.2 \times 10^{-22} \text{ mol}$. Therefore, there are 522 Ba and Ti atoms in $5 \times 10^{-16} \text{ cm}^3$ of the Kraton patch.

On a TEM grid 3 mm in diameter, the volume of the film is $4 \times 10^{-7} \text{ cm}^3$. Therefore, there are 4.416×10^{11} Ba and Ti atoms.

In a 50 nm × 50 nm × 50 nm BaTiO₃ cube with a unit cell dimension of 4 Å, there are 1.95×10^6 Ba and Ti atoms. Similarly, in a 10 nm sphere, there are ~8000 Ba and Ti atoms. If all Ba and Ti atoms in the film were liberated to form BaTiO₃ cubes and spheres, there would be 2.3×10^5 particles and 5.4×10^7 particles (1 sphere per area of 380 nm × 380 nm), respectively.

LA010525K

(44) Kunz, M.; Shull, K. *Polymer* **1993**, *34*, 2427.